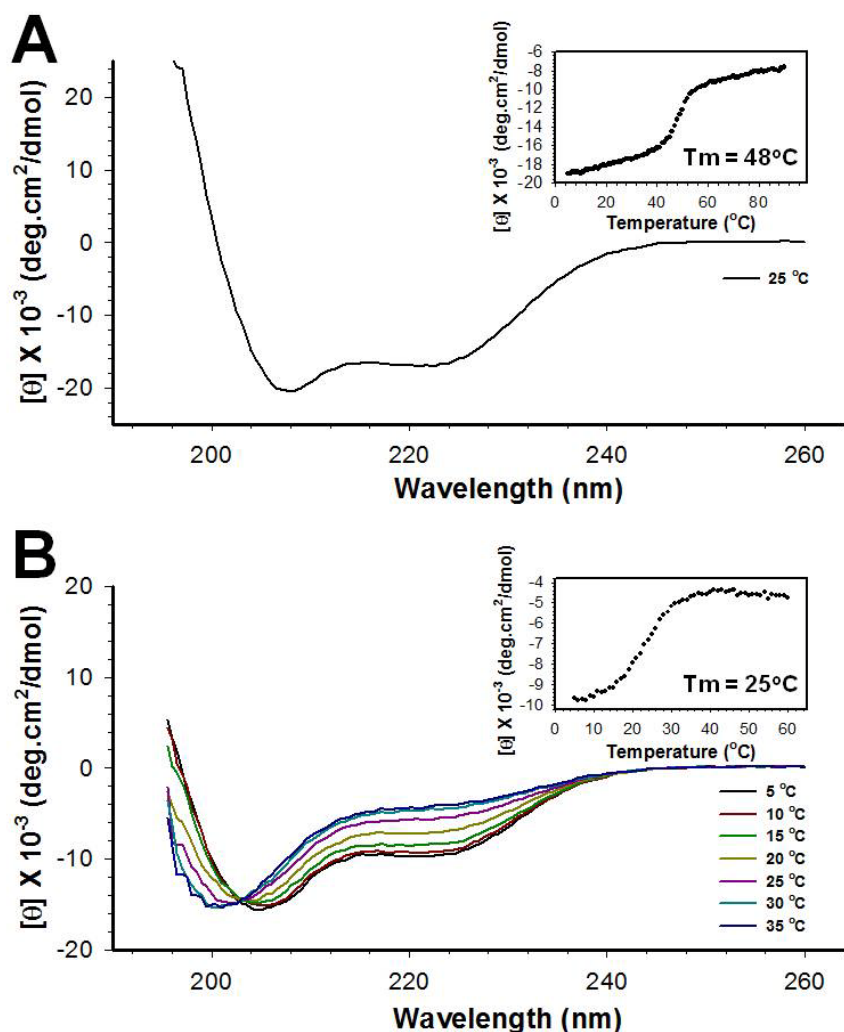


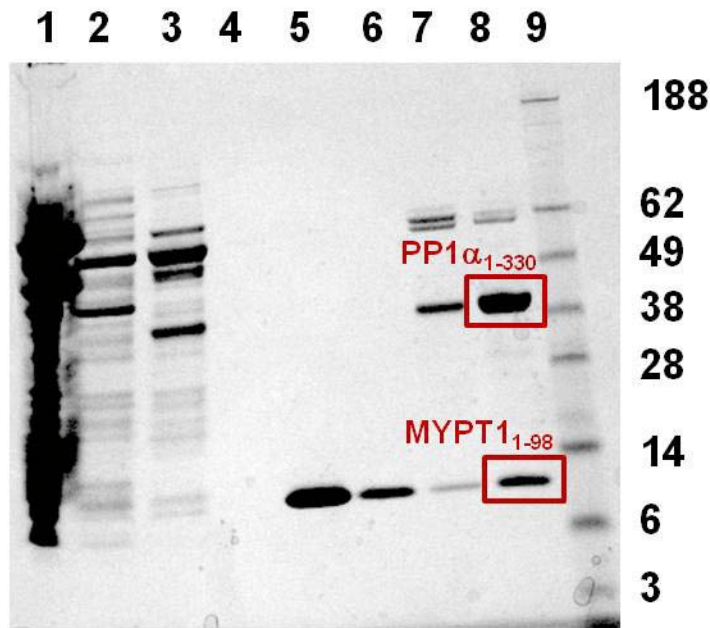
Supplemental Material

The Structural Signature of the MYPT1:PP1 Interaction

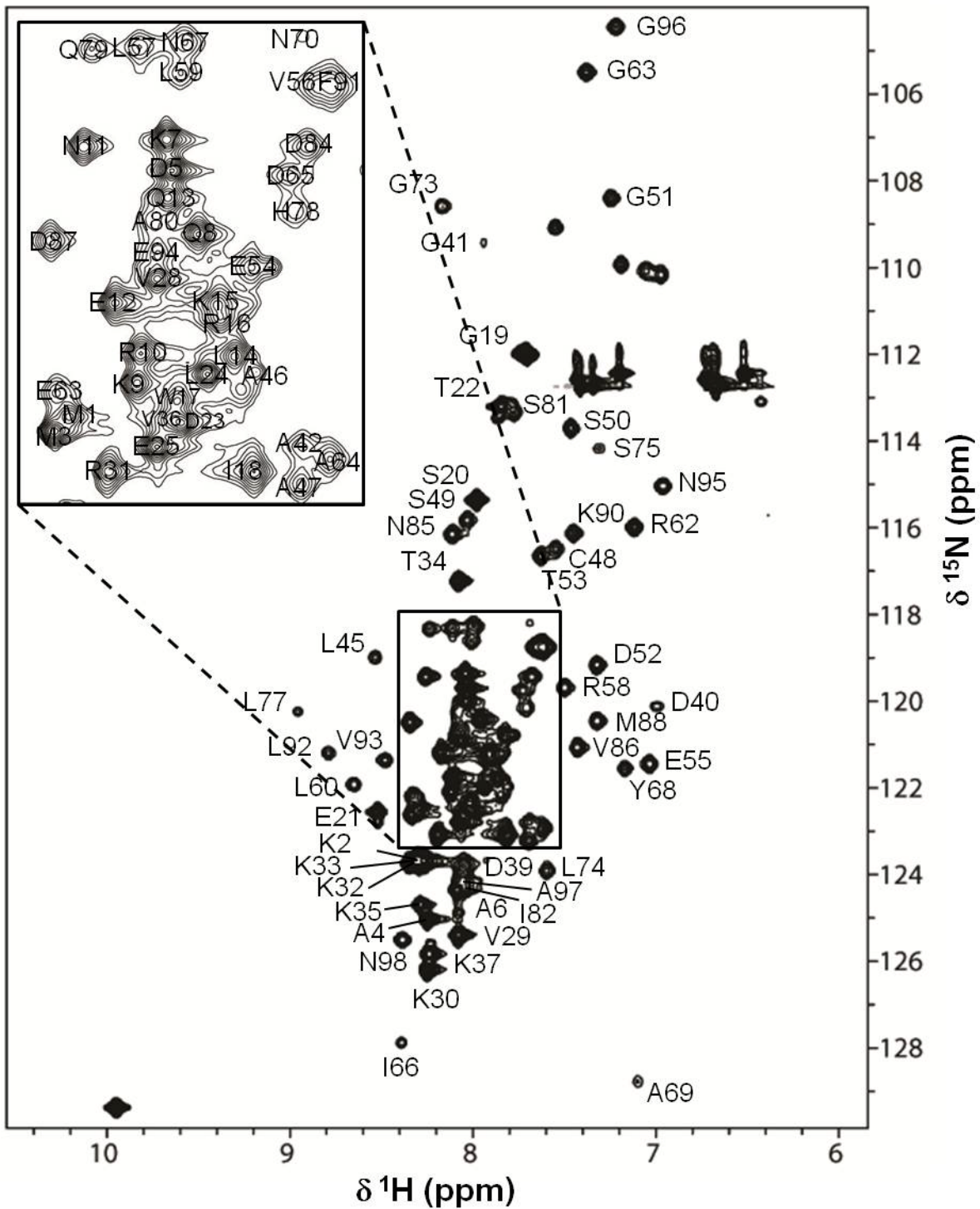
Anderson S. Pinheiro¹, Joseph A. Marsh², Julie D. Forman-Kay² & Wolfgang Peti^{1,§}



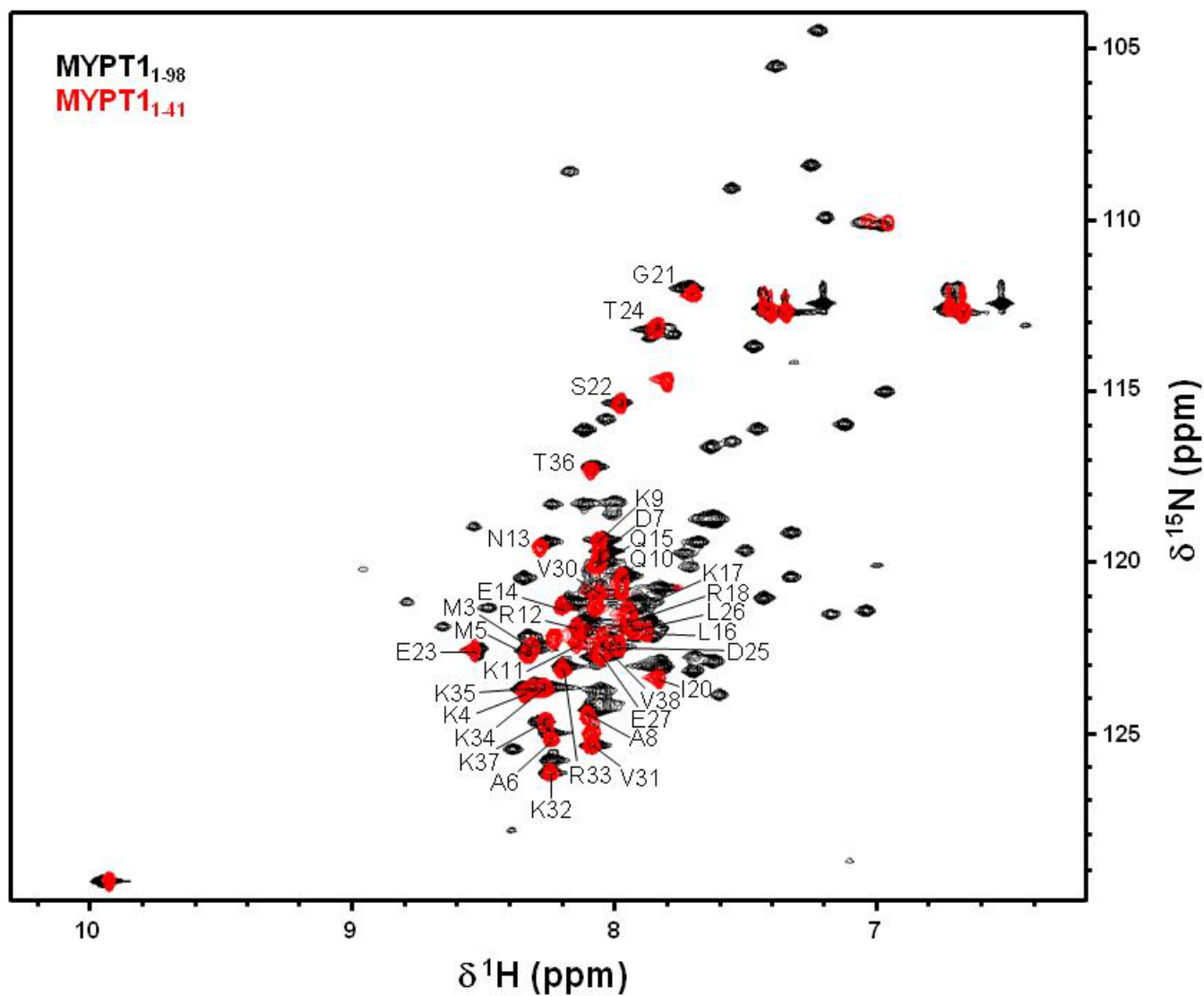
Supplemental Figure S1: Thermodynamic stability of MYPT1 constructs used in the studies. (A) Circular dichroism (CD) spectrum of MYPT1₁₋₂₉₉ recorded at 25 °C (20 mM Na-phosphate pH 6.8, 50 mM NaCl, 0.5 mM TCEP; sample concentration 5 μ M). The spectrum shows that expected hallmarks for an α -helical protein, with negative peaks at 222 and 208 nm. The insert shows a melting curve of MYPT1₁₋₂₉₉ recorded as a function of increasing temperature (measured @ 222 nm). MYPT1₁₋₂₉₉ has a melting temperature of \sim 48 °C. (B) Circular dichroism spectra of MYPT1₁₋₉₈ recorded at different temperatures ranging from 5 to 35 °C (identical conditions as A; sample concentration: 10 μ M). The stability of MYPT1₁₋₉₈ increases with decreasing temperature as shown by the migration of the negative peak in the CD spectrum from \sim 201 (random coil) to \sim 208 nm (α -helical). MYPT1₁₋₉₈ has a melting temperature of \sim 25 °C as shown in the insert.



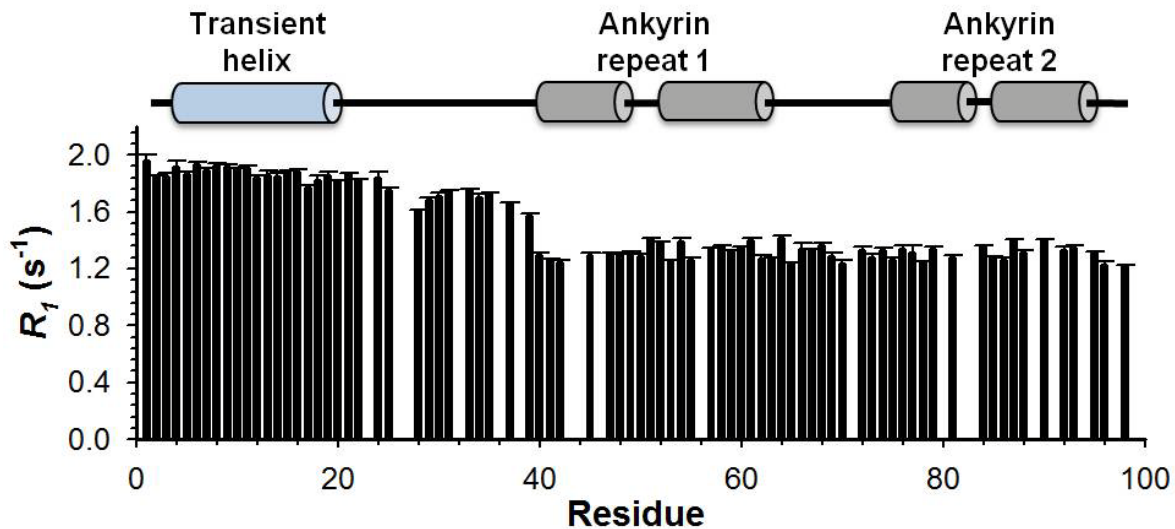
Supplemental Figure S2: MYPT1:PP1 complex formation. To experimentally verify the activity of MYPT1₁₋₉₈, we tested its ability to form a complex with PP1 α_{1-330} *in vitro*. Samples from different stages of the complex formation experiment were assayed by SDS PAGE as follows: (1) PP1 α_{1-330} flow-through, (2) wash with high salt buffer (50 mM Tris pH 8.0, 700 mM NaCl, 5 mM imidazole, 1 mM MnCl₂), (3) wash of PP1 α_{1-330} with 50 mM imidazole (50 mM Tris pH 8.0, 700 mM NaCl, 5 mM imidazole, 1 mM MnCl₂), (4) equilibration of the resin in low salt buffer (50 mM Tris pH 8.0, 50 mM NaCl, 5 mM imidazole, 1 mM MnCl₂), (5) flow-through of the incubation with purified MYPT1₁₋₉₈, (6) wash with low salt buffer, (7) wash with 250 mM imidazole (50 mM Tris pH 8.0, 50 mM NaCl, 250 mM imidazole, 1 mM MnCl₂), (8) elution of the MYPT1:PP1 complex with 500 mM imidazole (50 mM Tris pH 8.0, 50 mM NaCl, 500 mM imidazole, 1 mM MnCl₂), (9) molecular weight marker. Co-elution of His₆-PP1 α_{1-330} (~ 40 kDa) and MYPT1₁₋₉₈ (~ 11 kDa), as indicated by the red boxes and corresponding labels, confirms successful complex formation.



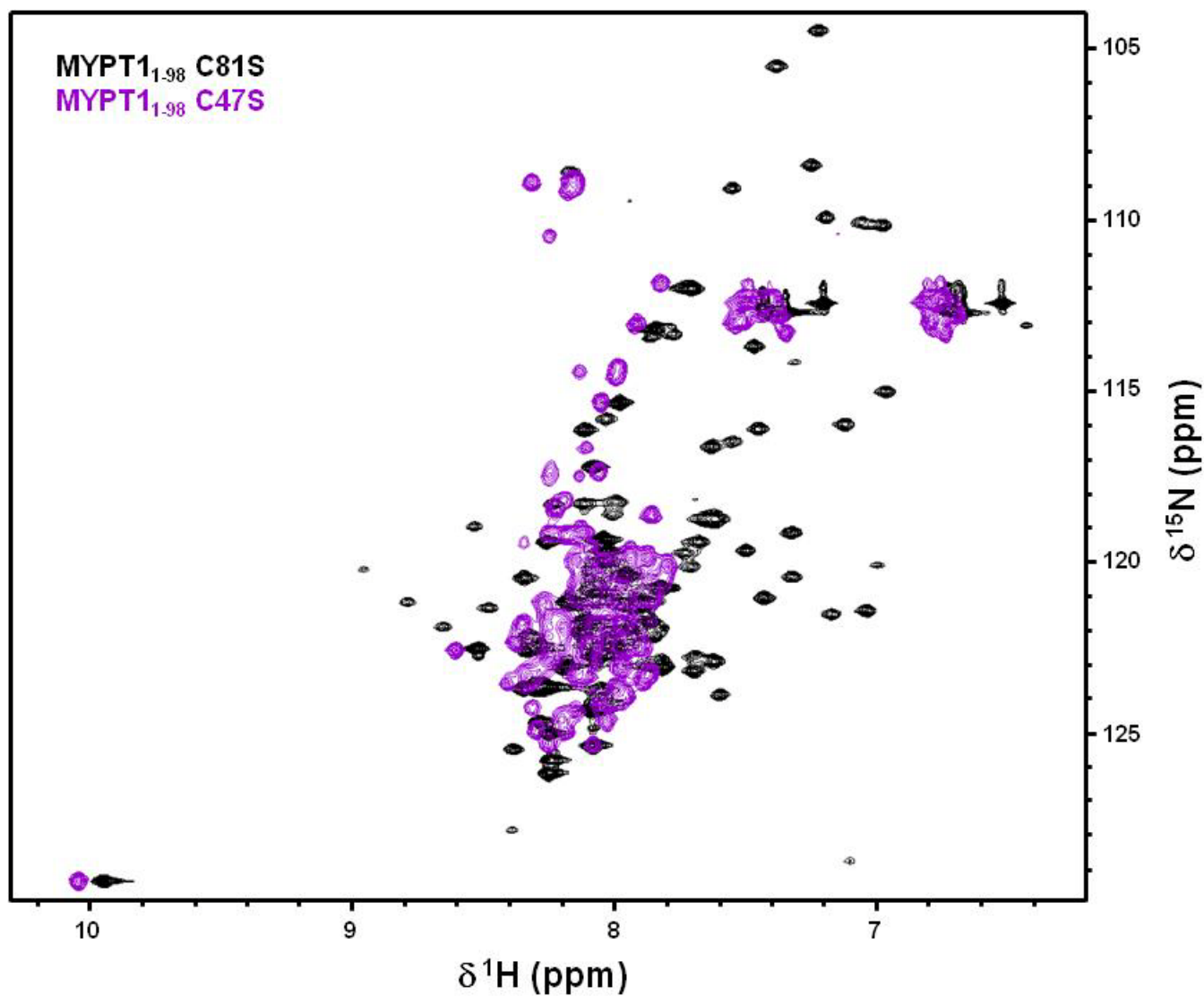
Supplemental Figure S3: Fully annotated 2D [^1H , ^{15}N] HSQC spectrum of MYPT1₁₋₉₈. Residues were marked with their residue name (one letter code) and number in protein sequence.



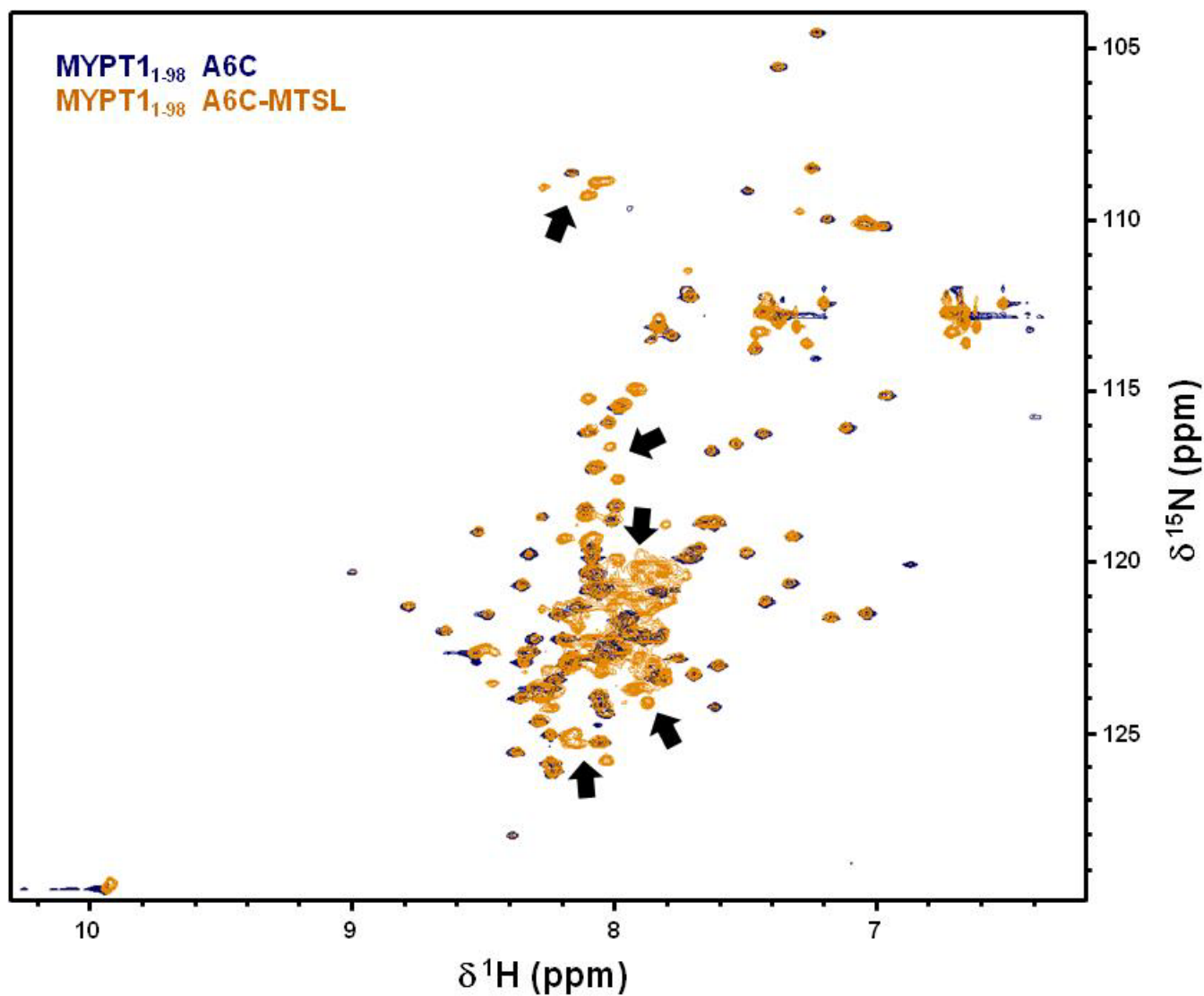
Supplemental Figure S4: Superposition of the 2D [^1H , ^{15}N]-HSQC spectra of MYPT1₁₋₉₈ (black) and MYPT1₁₋₄₁ (red). Both spectra were acquired using identical sample concentration (0.5 mM), buffer (20 mM Na-phosphate pH 6.8, 50 mM NaCl, 0.5 mM TCEP) and temperature (278 K). H^{N} , N chemical shifts of MYPT1₁₋₄₁ overlap exceedingly well with those of MYPT1₁₋₉₈ confirming the independent behavior of these two domains. MYPT1₁₋₄₁ residues are annotated.



Supplemental Figure S5: MYPT1₁₋₉₈ ^{15}N R_1 relaxation rates plotted as a function of the protein sequence. The two-domain behavior showed by MYPT1₁₋₉₈ is reflected by the relaxation rates. The N-terminal PP1-binding domain shows less restricted backbone motions than the C-terminal ankyrin-repeat domain, as indicated by higher R_1 values. Secondary structural elements, based on the MYPT1:PP1 complex structure is shown as cartoon representations.

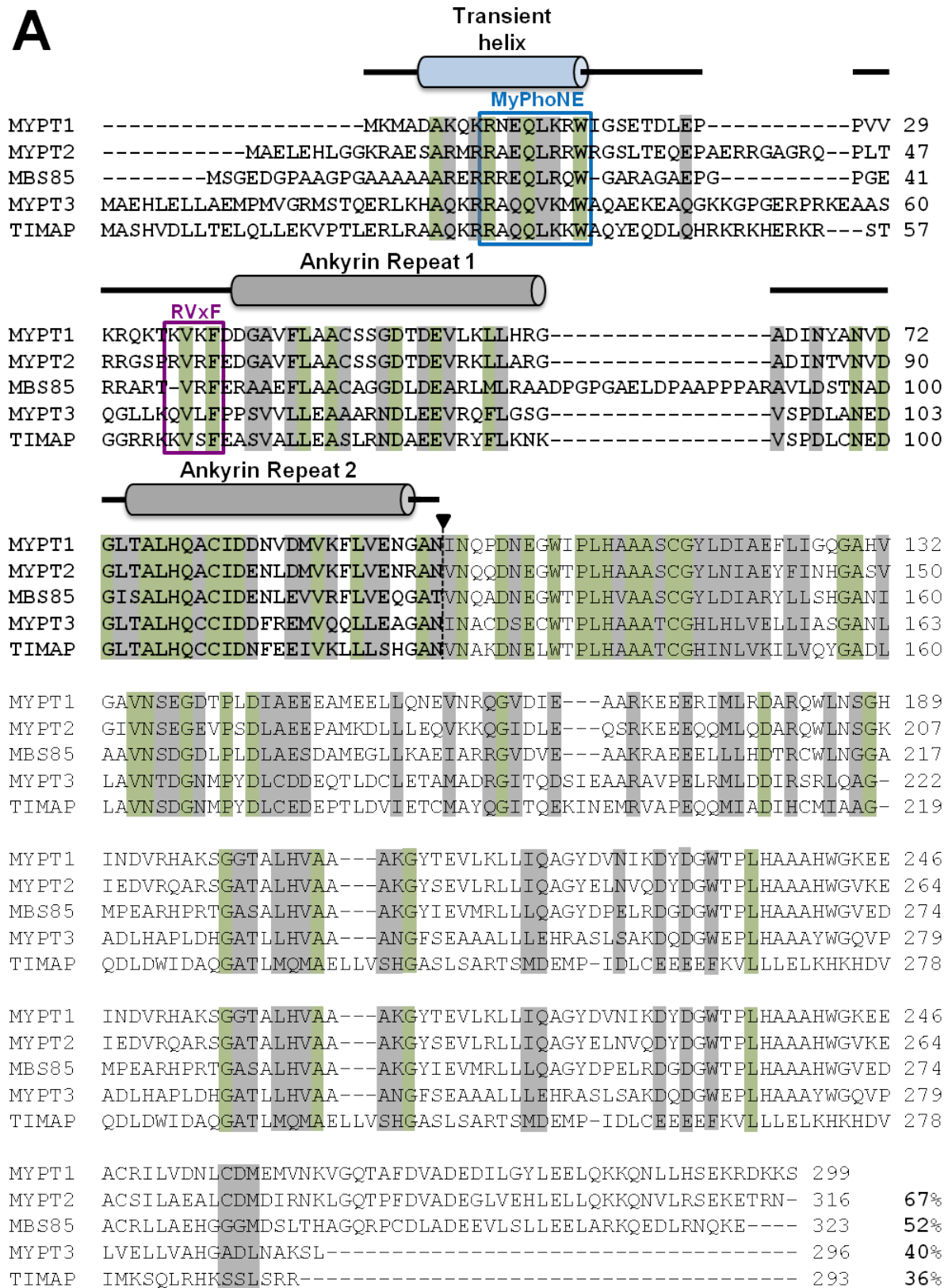


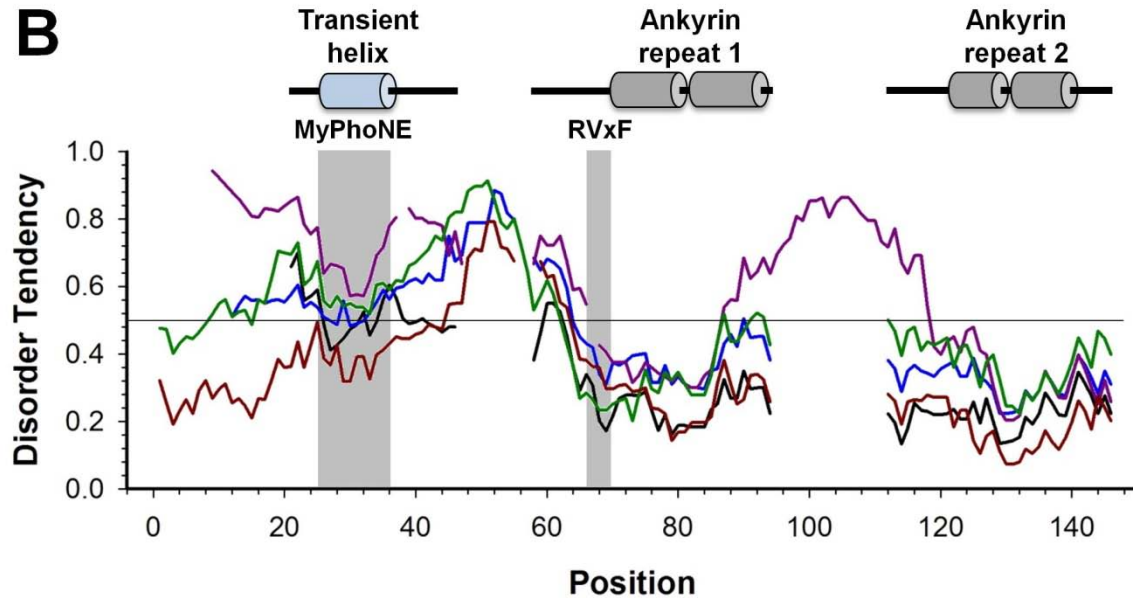
Supplemental Figure S6: Effect of the mutation of cysteine residues on the overall structure of MYPT1₁₋₉₈. Superposition of the 2D [¹H, ¹⁵N]-HSQC spectra of MYPT1₁₋₉₈ C81S (black) and MYPT1₁₋₉₈ C47S (purple). Experimental conditions are identical to those described in **Supplemental Figure S4**. Mutation of Cys47 to Ser disrupts the packing and thus folding of the ankyrin repeats, as shown by the disappearance of the well-dispersed NH cross-peaks in the MYPT1₁₋₉₈ C47S spectrum (purple).



Supplemental Figure S7: Superposition of the 2D [¹H,¹⁵N]-HSQC spectra of MYPT1₁₋₉₈ A6C (blue) and MYPT1₁₋₉₈ A6C-MTSL (orange). Experimental conditions are identical to those described in **Supplemental Figure S4**. Labeling of MYPT1₁₋₉₈ A6C with MTSL leads to the appearance of a new set of cross-peaks in the 2D [¹H,¹⁵N]-HSQC spectrum, indicated by multiple arrows. This suggested the existence of an additional conformation in solution and made the use of the paramagnetic label impossible.

A





Supplemental Figure S8: (A) Primary sequence alignment of human MYPT1 (residues 1-299) and its isoforms MYPT2, MYPT3, MBS85 and TIMAP (order is based on sequence identity). Identical residues are highlighted in green, similar residues are shaded in gray. The two consensus PP1 binding motifs, MyPhoNE and RVxF, are depicted by blue and violet boxes, respectively. MYPT1₁₋₉₈ and corresponding primary sequences in MYPT2/3, MBS85 and TIMAP are highlighted in bold. Secondary structural elements, based on the MYPT1:PP1 crystal structure, are shown using cartoon representations. (B) Comparison of disorder tendency among members of the MYPT family. The disorder tendency was predicted using the program IUPred. Values of disorder tendency were plotted according to the primary sequence alignment in Figure S8A. In the graph: MYPT1 (black), MYPT2 (blue), MBS85 (violet), MYPT3 (green) and TIMAP (red). A disorder tendency above 0.5 suggests regions with higher propensity for disorder. The two PP1 consensus binding motifs, MyPhoNE and RVxF, are highlighted by gray boxes. Secondary structural elements, based on the MYPT1:PP1 crystal structure, are shown using cartoon representations.